Modeling Heat Exchange in Spatial Steering of Deep Brain Stimulation

BEE 4530

Group 11

Matthew Mitchell, Khalid Barghouthi, Mihailo Rebec

Table of Contents

EXECUTIVE SUMMARY

Deep brain stimulation (DBS) is a treatment that involves insertion of a probe and stimulation of brain tissue with an electric potential (or injection of current). Electrical stimulation has been demonstrated to be an effective treatment in a variety of neurological conditions, serving to relieve motor-symptoms and tremors in advanced stage Parkinson's disease and Essential tremor. Current DBS therapy involves electrically stimulating a specific region of the brain symmetrically about the probe lead via pulses of electrical potential. Currently-used leads apply potential symmetrically about the cylindrical probe's central axis. This, however, is problematic, since stimulation needs to be highly specific, yet there is little that can be done to alter the applied electric field after the probes have been implanted. Asymmetric stimulation, on the other hand, allows increased control over direction within these complex regions of the brain, affording more targeted stimulation following the implantation procedure. A problem with any form of electrical stimulation, however, is heating. Even a 1 °C change in temperature can cause adverse effects due to strong membrane potential and pump kinetics dependence on temperature. Heat is generated due to both Joule heat from the applied potential and through increased metabolism rates caused by physiological shifts in neurons influenced by the stimulation. Our project focused on creating a computer model of electrothermal deep brain stimulation utilizing a novel probe design based upon the one proposed in Martens, *et al* in order to ensure safety and efficacy of this probe.

We created a 3D model in COMSOL representing a probe capable of asymmetric heating. A symmetric configuration of our model showed a similar temperature distribution to both computational models and experimental measurements made by Elwassif *et al*., as well as a similar electric potential profile to models by Martens, *et al*, demonstrating validity of our computational model. Stimulation due to asymmetric stimulation showed almost no significant temperature increase in the unstimulated direction when the probe was asymmetrically activated, and ultimately ensured safe deep brain stimulation and effective temperature and voltage control.

The sensitivity analysis showed that voltage was the most important factor for temperature distribution. Because of this, we believe that optimization should be based on an individuals' symptoms and geometry at which the probe is implanted. Models like ours lead to better understanding of heat distribution under asymmetric stimulation and more affective deep brain steering stimulation, ultimately leading to higher success rates for suffering neurological conditions and decreasing likelihood of brain damage.

INTRODUCTION AND PROBLEM STATEMENT

A. Background:

Deep Brain Stimulation (DBS) is a novel treatment method capable of providing dramatic clinical relief to those suffering from a variety of neurological conditions—most notably, to those with Parkinson's disease (PD) or Essential tremor (ET). While chronic electrical stimulation had been explored as a treatment method for neurological conditions since the 1960s, it didn't become widespread in treatment of any disorder until the 1990s. Lesioning is the targeted destruction of brain cells to reduce tremor-related symptoms and was the primary surgical treatment for PD prior to new non-surgical levodopa treatment options. The 1990 results by Alexander and Crutcher, among others, demonstrated the efficacy of high frequency electrical stimulation of different brain structures in treating neurological conditions, paving the way for modern DBS treatments. The first widespread use of DBS for treatment of ET and PD followed the 1991 Benabid, *et al* publication, which demonstrated efficacy of chronic stimulation of ventrointermediate nucleus of the thalamus in the treatment of tremors (Breit, *et al.*). Soon, DBS of the subthalamic nucleus (STN) was perceived as an increasingly viable treatment method for PD. DBS quickly proved to be among the most promising therapies for advanced PD by the turn of the millennium because it allows for post-operative fine-tuning of dosage and excludes destruction of brain tissue (Perlmutter & Mink).

B. Research Review/Literature Review:

Results have shown STN DBS to be effective in reducing motor-related symptoms of PD. (Perlmutter & Mink). Effects of stimulation of different structures is still under investigation. DBS is also increasingly employed as a treatment option for a number of psychological and neurological conditions, including Dystonia, Tourette syndrome, Depression, and Obsessive Compulsive Disorder (Perlmutter & Mink). The physiological mechanisms that allow DBS to function are many and vary by disease, brain structures stimulated, and type of stimulation, but functions, in general, through disruption of the native firing patterns of groups of neurons responsible for symptoms of these disorders (Kert, *et al*). While DBS is an efficacious treatment for a variety of disorders, it does have its risks.

Electrical stimulation of brain tissue can heat these tissues due to changes in metabolism of stimulated cells, as well as through Joule heating. While the heating may be minimal, even a 1 °C shift can impair neuronal function (Elwassif, *et al*). Elevation in temperature may even mitigate the desired effects of DBS by affecting the behavior of voltage-gated ion channels and pumps. Blood perfusion rates may also change. In order to explore DBS tissue heating Elwassif, *et al* modeled temperature changes in response to stimulation using the Model 3387 DBS lead and the Model 3389 DBS lead. While these leads, manufactured by Medtronic, Inc., remain the gold standard for such procedures, emerging technologies need also be considered. One such promising technology is the probe proposed by Martens, *et al.*, which allows asymmetric stimulation of brain tissue. Such a technology would allow more specificity and postoperative control in a treatment that is known to be highly sensitive to electrode placement. Because of the considerable advantages such a lead could offer, it is important to explore its temperature-related effects on the brain and stimulation patterns to ensure both its efficacy and safety.

C. Current Research:

Our project involves a computational model of this asymmetric stimulation of brain tissue, which was created using COMSOL. The goals for our model is to simulate heat changes and the electric potential around an active probe, stimulating brain tissue. Another important guideline is to prevent damage of brain tissue by ensuring that temperature variations do not exceed the proposed critical temperature of 38 °C. By successfully creating a model of asymmetric deep brain stimulation we hope to show that the procedure could be optimized in order to increase the precise control of the stimulation, decrease likelihood of brain damage, and subsequently increase the number of patients who experience significant symptom relief.

DESIGN OBJECTIVES

- Model the heating of brain tissue, considering both Joule heating and the metabolic increase in affected neurons.
- Initially simulate the symmetric stimulation case to validate our model and ensure that this configuration is representative of current methods of DBS.
- Show that the modeled probe is safe in asymmetric activation of electrodes, by confirming minimal temperature increases associated with its use and demonstrating that this probe is able to offer greater control of its stimulation than its predecessors.

MODEL FORMULATION

A. Geometry/Schematic:

This study modeled the heat transfer of DBS in three dimensions through brain tissue by applying the governing heat transfer equation for a 3-D Cartesian geometry using COMSOL. The brain tissue properties were assumed to be homogeneous. The modeled probe was a simplified design of the probe proposed in Martens, *et al.* Instead of having 16 rows of four electrodes, four rows of four electrodes were used in the study. The shape of the electrodes were also changed, from circles to squares of the same area. These simplifications were made to make modeling simpler and to recognize that early versions of probes of this type are likely to be simpler in design. This will be discussed in further detail in the last section of the paper. It was also assumed that this probe is constructed from the same materials as those used in the state-of-the-art brain probes and that the material of the probe is a function of its angle, so that the cross-section of the materials is as pictured in Fig. 3. The surrounding brain tissue was modeled as a semi-infinite cylinder, which was taken to be coaxial with the probe with a radius of 50 mm. Distances between electrode points, probe length, brain tissue diameter can be found in Fig. 1.

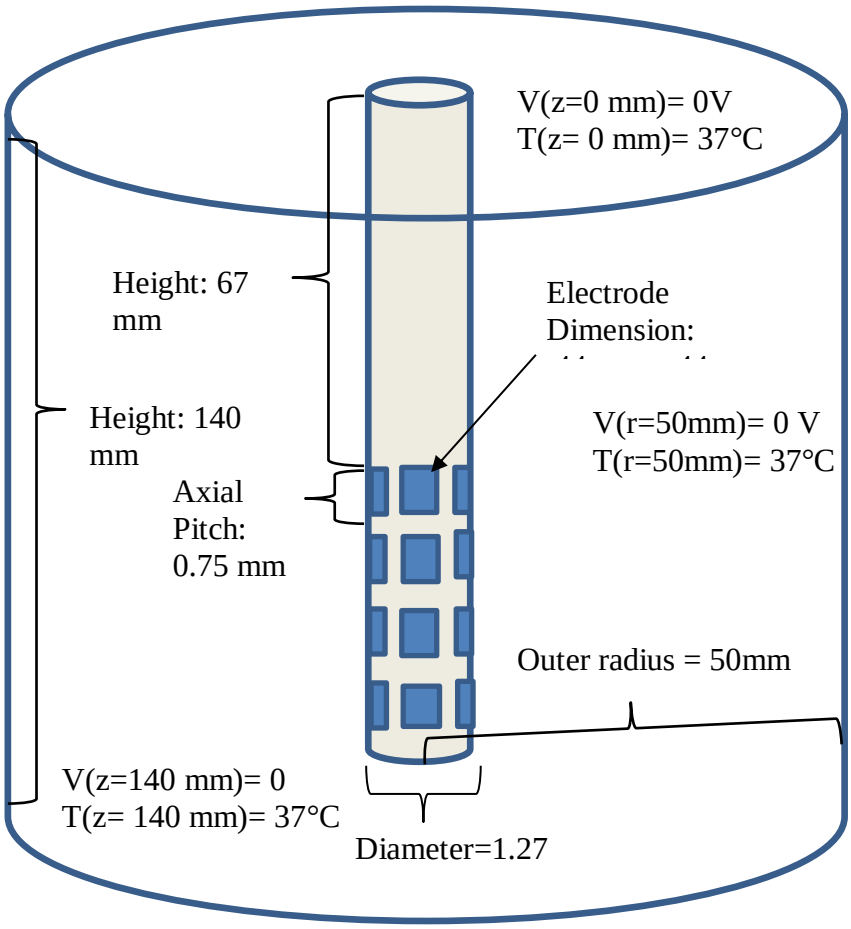

Figure 1: Geometry and parameters of the probe.

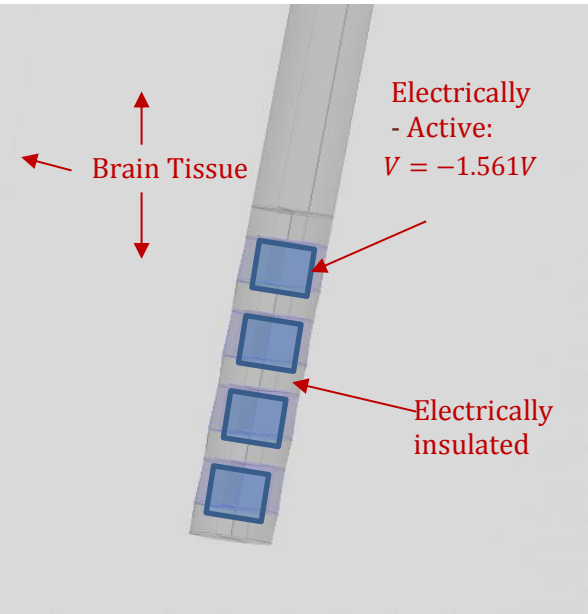

Figure 2: Schematic Computational domain of interest is the region surrounding the probe. The probe is located in the middle of the cylinder. Boundary conditions include electrically active and insulated parts of the probe.

Using this model, the standard temperature profile involves applying -1.561 V for 15 minutes at the electrically active portions of the probe, as shown in the COMSOL model of the probe, pictured in Fig. 2. The brain tissue surrounding the probe simulates the changes in temperature due to changes in metabolism and Joule heating. More information about the governing equations and parameter values may be found in Appendix A. Information relating to the COMSOL-related computational methods and solving procedures may be found in Appendix B.

SYMMETRIC STIMULATION

A. Results:

A temperature profile in regions around the probe was found by symmetrically activating the bottom two rows of the probe over 15 minutes. The temperature profile at the final time can be seen in Fig. 3.

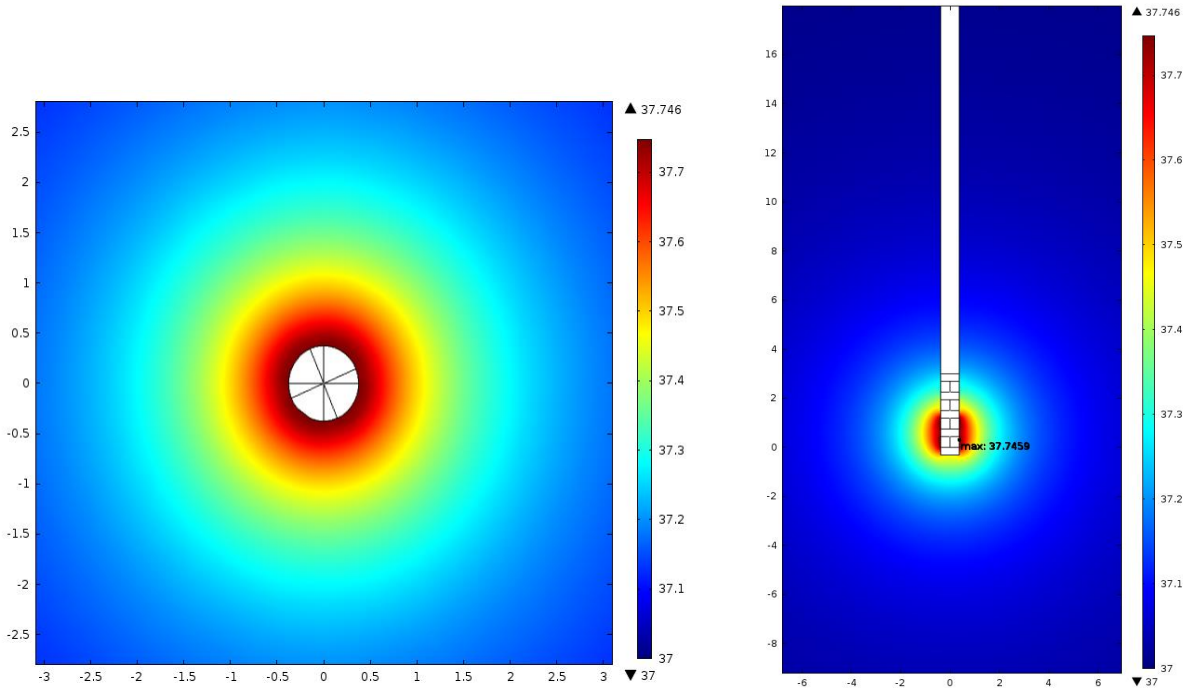

Figure 3: Surface plots of temperature distribution in model after 15 minutes. a) x-y plane (slice through z-axis) b) y-z plane (slice through x-axis).

It is clear from Fig. 3 that the temperature remains roughly constant as the distance increases from the probe, after some distance far enough out from the boundary of the probe. Concentrated heating, on the other hand, can be found in the regions where the brain tissue is in contact with the probe. Fig. 3 shows that heat travels radially outward, with temperature highest at the surface of the probe.

Part of the purpose of exploring the results of symmetric stimulation is to have results against which to compare the effects of asymmetric stimulation. It allows us to validate our model with other groups' models and experiments, thereby also allowing the use of this symmetric stimulation case (in which the bottom two rows of the probe are active) of our model as a proxy for the currently-used probes. This validation will be explored in the next section.

B. Model Validation:

In order to check the accuracy of our model and let the symmetric stimulation case serve as a viable representation of current probe options, the final temperature of our model under which the bottom two rows were completely activated was compared with data obtained from a study using a traditional symmetrical probe by Elwassif, *et al*. This study shows experimental findings of temperature variations near the probe using the traditional probe in DBS. The model's parameters were matched to those in the study to confirm the accuracy. The metabolic heat generation and blood perfusion were set to zero, as they were in this part of the study. The same run-time of 15 minutes was also used. Temperature profiles from the studies can be found below.

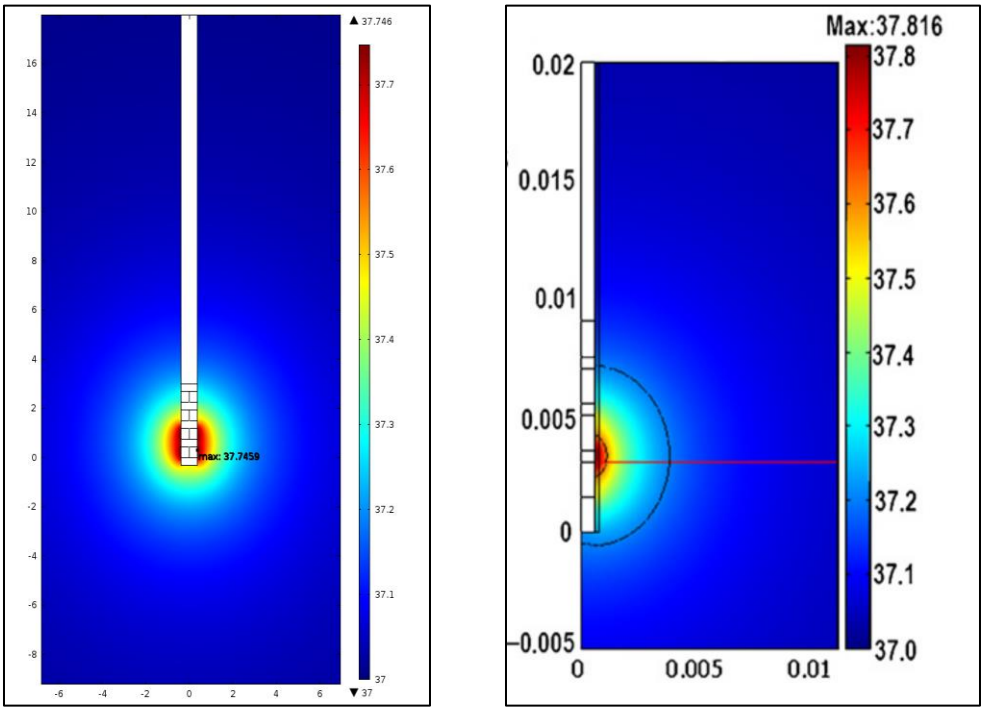

Figure 7: Surface plots of temperature distribution. a) y-z plane (slice through x-axis) for our model b) obtained temperature profile from Elwassif, *et al*: These plots contain a visual representation of the temperature distribution within the brain tissue surrounding the probe.

The temperatures observed in our model were very close to the temperatures from the experiment conducted in the literature. The maximum temperature was found to be 37.75 degrees Celsius for our model, compared to 37.82 degrees found in the study performed by Elwassif, *et al*. We also validated our model using the results of work by Martens, *et al.*

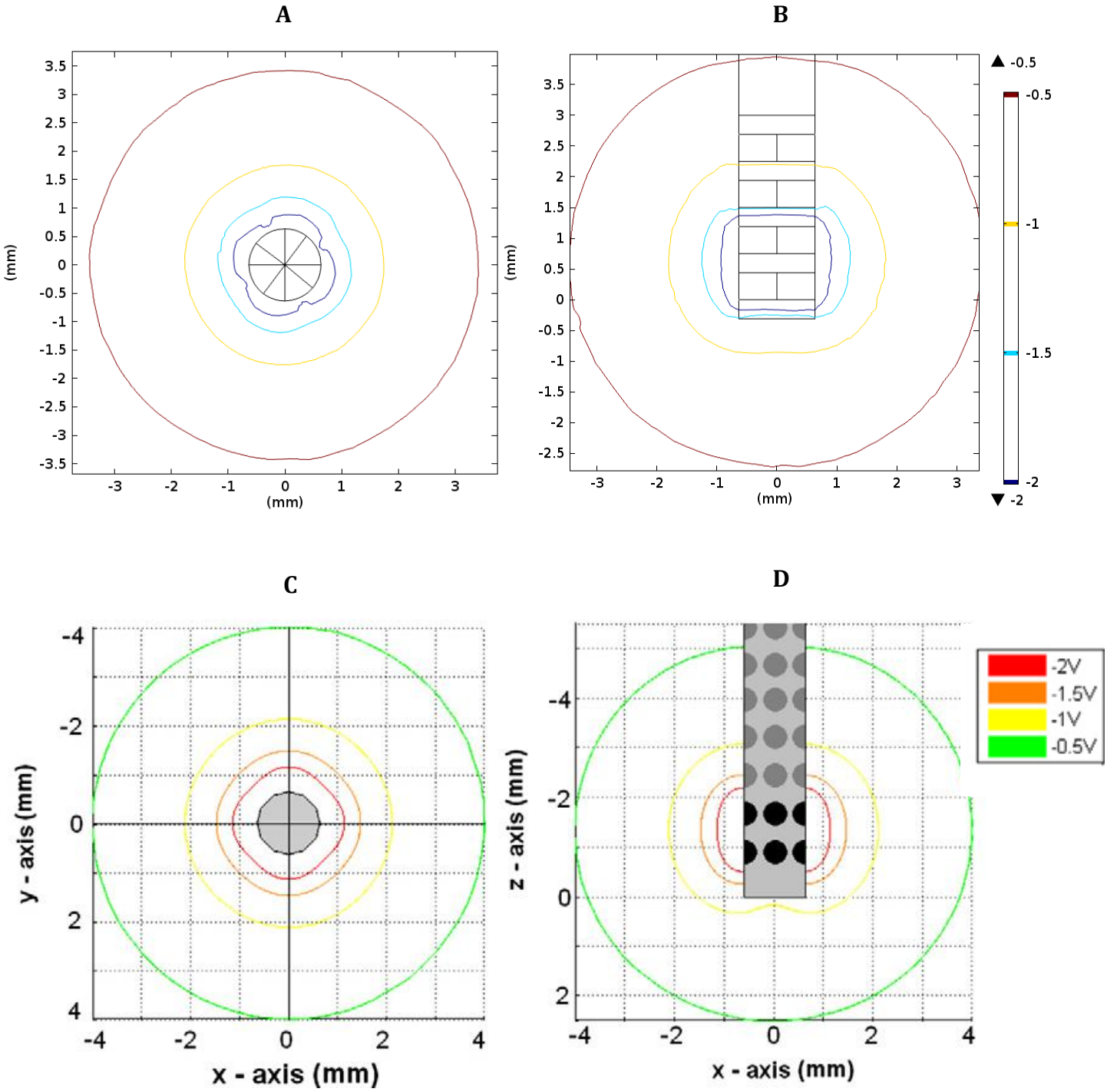

Figure 12: A and B show a contour plot of the potential at 4 levels under the same conditions (conductivity of the surrounding area set to .1 S/m) as those presented in Martens, *et al.* C and D shows their results in each case for the modeled probe. A and C correspond to voltages on the cross-section, while B and D are potentials of a vertical plane through the center of the probe.

The voltages of the model were also compared to those waveforms solved in Martens, *et al.* In this paper, the novel probe off which our model was based and the older probe are shown to have the same lines of constant voltage. This time, the active electrodes (the bottom two rows again) are set to -3V and the electrical conductivity of the material surrounding the probe is modeled as 0.1 S/m (This value was used by the group to compare potential functions in space and is not meant to be the conductivity of brain tissue). Comparing results, it is evident that the equipotential lines are very similar. The lines in the model correspond approximately to circles that are slightly smaller in diameter than those found by this group. This may be because the electrode was not modeled as shielded or insulated, but as having very small conductivity. It may also be because the electrodes in the case of our study are square, while theirs are circles that we see this slight difference. Additionally, it may simply be a matter of a difference in the relative positioning of the planes that were selected. In any case it seems that the model is accurate.

C. Sensitivity Analysis:

The sensitivity analysis focused on evaluating the temperature dependency of the brain tissue on a few of the parameters that are not known to be constant. Parameter sweeps aided to see how different values affected the temperature, after steady state had been achieved. The metabolic heat generated from stimulated neurons can vary widely from 5000 W/m^3 to over 15000 W/m^3. Even with this wide range, the maximum difference in temperature between the three values is only about 0.2 °C over the entire length. Blood perfusion rate can vary from patient to patient, which can lead to values ranging from .004 to .012 $mL/s\ cm^{-3}$. This parameter sweep showed that the temperature profile depends negligibly on the blood perfusion rate, with a maximum difference of about 0.1 degrees. Parameter sweeps were also performed on the thermal and electrical conductivities. The resulting changes in temperature profiles as a function of distance from the probe are shown in Fig.8.

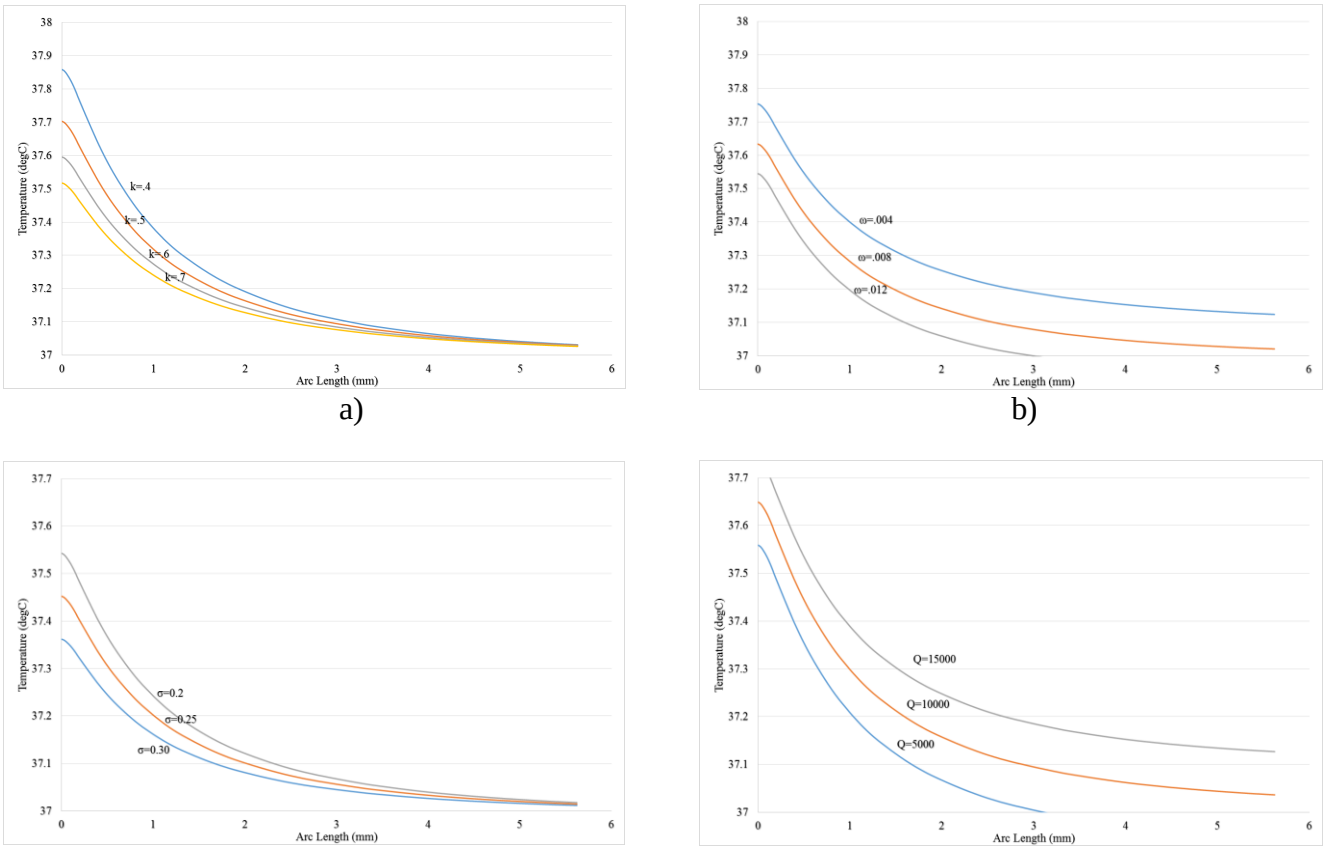

Figure 8: Line graphs of temperature distribution for brain tissue located radially outward in the horizontal direction. (See Appendix C, Fig. 1.) a) varying thermal conductivity values b) varying blood perfusion rate values c) varying electrical conductivity values d) varying metabolic heat generation values: These plots contain a visual representation of the temperature distribution within the brain tissue surrounding the probe, under varying certain material properties. Larger versions of each plot can be found in Appendix C, Fig. 2.

Based on the results from the sensitivity analysis for blood perfusion rate, metabolic heat generation, electrical conductivity and thermal conductivity, the temperature is not significantly affected by reasonable variation in any one of these parameters. There is less than a single degree difference between the two most extreme values in all four cases. These moderate increases in temperature are in line with what is expected and is considered to be of minimal risk. Unless a number of parameters is in reality much higher than the literature suggests, the results indicate that stimulation with the probe would be safe for a wide range of patients. Even though tissue properties vary between patients and within brain structures, the model supports that there will be little difference in temperature change associated with these differences in all but the most extreme situations. The problem now shifts to one of optimization: designing the optimal activity configuration for steering the potential function (depending, in practice, on the patient's symptoms and geometry at which the probe is implanted) and ensuring its safety. Personalized treatment could be used to optimize treatment by directional stimulation of desired brain tissue based on a patient-to-patient basis.

ASYMMETRIC STIMULATION

A) Optimization: Results and Discussion:

Now that the model has been validated, we began to explore the safety and efficacy of different types of asymmetric stimulation. In this case, all electrodes in two adjacent columns of the probe were activated, and the result of stimulation for 15 minutes are shown in Fig. 4.

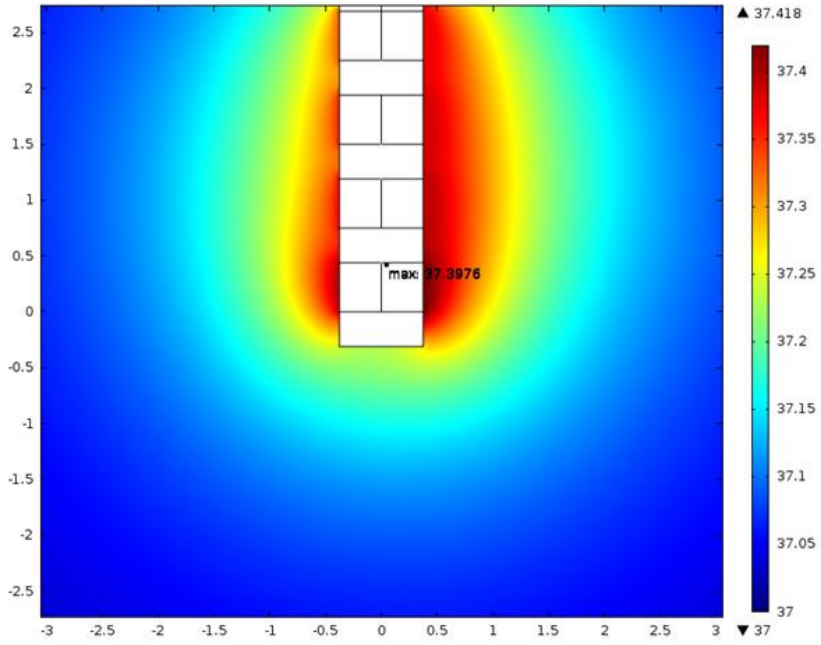

Figure 4: Surface plot of temperature distribution with two-column activation after 15 minutes.

It is clear from Fig. 4 that temperature increases the most on the side where the columns are activated. A maximum temperature of 37.4 °C was observed, which is lower than what was found when stimulating symmetrically. Because this configuration has been found to be safe, as the change in temperature was smaller than the allowed, the extent of spatial steering can now be considered. Contour plots for the voltage variation across the brain tissue for both the symmetric and asymmetric are shown in Fig. 5.

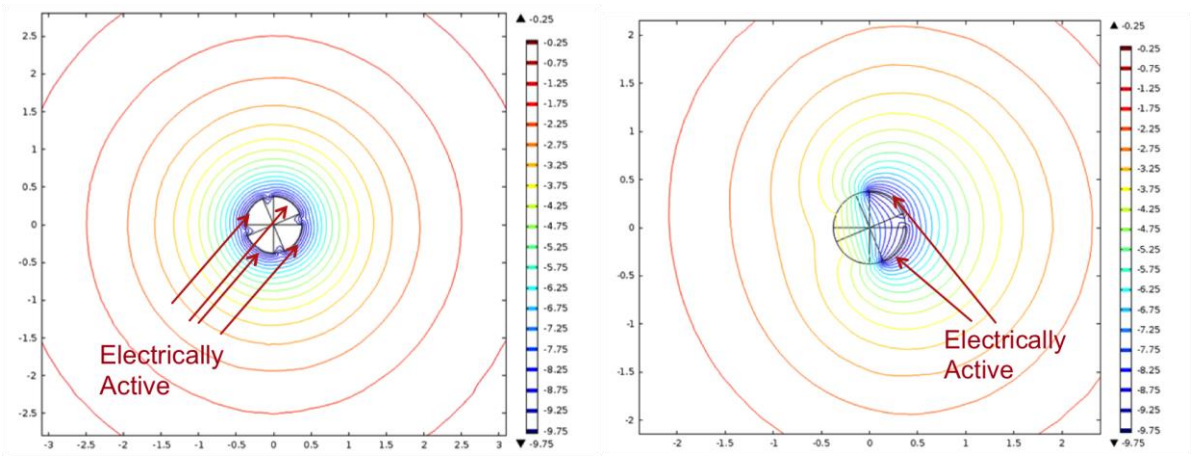

Figure 5: Contour plots of voltage distribution, setting the voltage at the surface of the probe to be -10 V, --its peak in the stimulation pulse, to more clearly see differences between the two. a) Shows symmetric activation b) shows the asymmetric activation configuration described above, with each plotting equipotential lines in a cross-section of the probes.

It is clear from Fig. 5 that voltage variations can be specific in a certain direction, depending on how the probe is being activated. Fig. 5 shows directional stimulation with little propagation in the unstimulated direction. To consider this more carefully, a projection analysis was performed wherein all points with a z-coordinate within 4mm of the active electrode part of the probe were projected down into the xy-plane. Next, those with radii greater than 5mm were excluded. Finally, all the points near the probe were divided into groups, based upon their angle measure from the positive x-axis. There were 50 groups corresponding to 50 equal partitions of this angle which varied, of course, from 0 to 2π. The average of these points in each set was taken and a more quantitative analysis of optimization of directional stimulation, in terms of voltage, was obtained. The results of this analysis is shown in Fig.9 below.

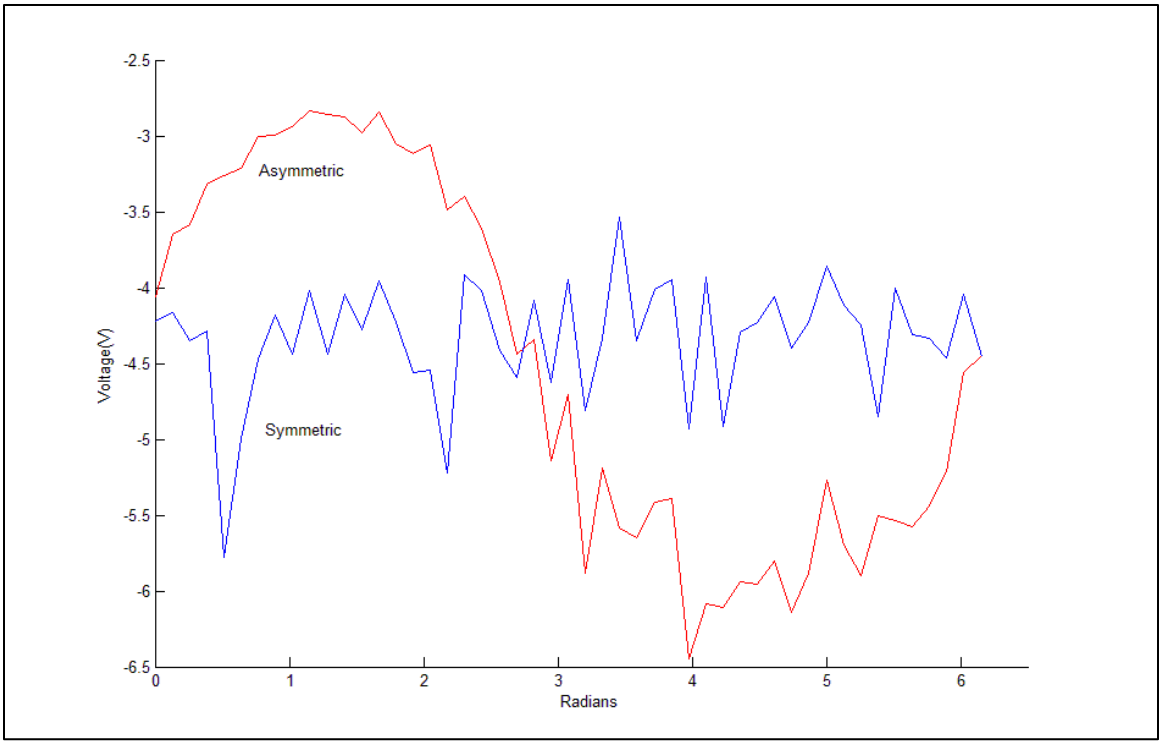

Figure 9. Voltage vs radians: Quantification of the stimulation around the probe in symmetric and asymmetric stimulation.

From the graph we gained a good understanding of the effectiveness of directional stimulation. It was important to measure the variance in each of the findings in order to better analyze the effectiveness of directional stimulation. We found that the variance in the data for the asymmetric activation was 1.478, compared to 0.153 for symmetric activation of the probe. A smaller variance corresponds to less change of the voltage with the angle. Because the asymmetric configuration had a much larger variance than the currently used model, these results further support that there is indeed diminished voltage propagation in the undesired direction.

These results give a way to further investigate more complex variations of electrode activation. For example, the electrodes can be activated in a specific pattern when a smaller gradient is desired. Accordingly, we performed an analysis with two activated rows in each column separated by an inactive row, as shown in Fig. 10. This study was again compared to the symmetric condition. Our findings of voltage variations of the given symmetric and asymmetric situations are shown in Fig. 6.

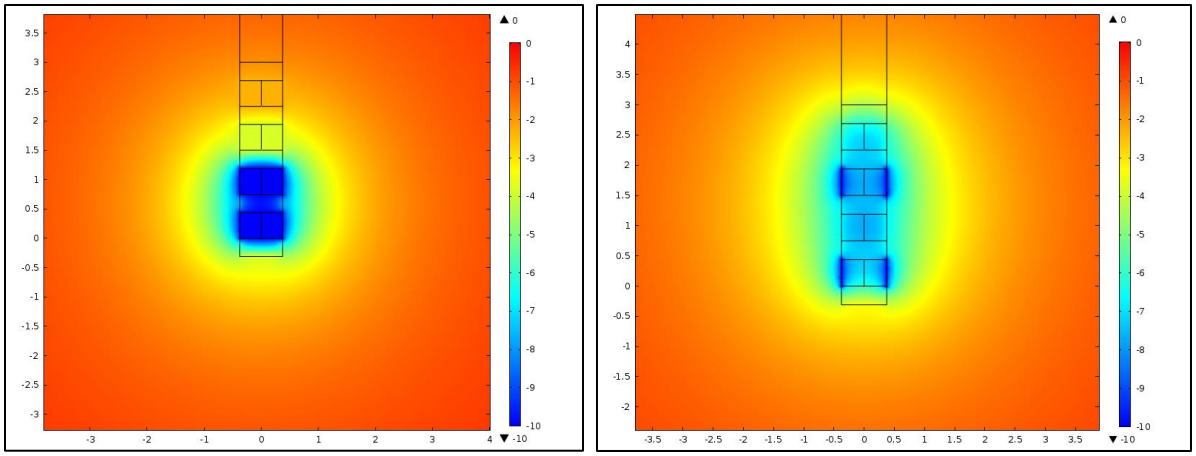

Figure 6: Surface plots of voltage distribution in model after 15 minutes. a) bottom two adjacent rows are activated b) two activated half rows separated by an inactive row: These plots contain a visual representation of the voltage distribution within the brain tissue surrounding the probe.

It can be seen from Fig. 6 that electrode configurations with asymmetric activation can produce propagation of the potential outward with a smaller gradient. In order to stimulate the same number of neurons, compared to previous models, a lower potential could be used due to the larger stimulation volume produced in this configuration. Lower voltages would in turn, lower the temperature overall in the brain tissue, reducing risk significantly.

In order to quantify this relationship, the same method of analysis as that utilized in Fig. 9 is used to consider the electric potential as a function of the radius (dividing the radius into 50 ranges, this time). The results of this analysis are shown in Fig. 11.

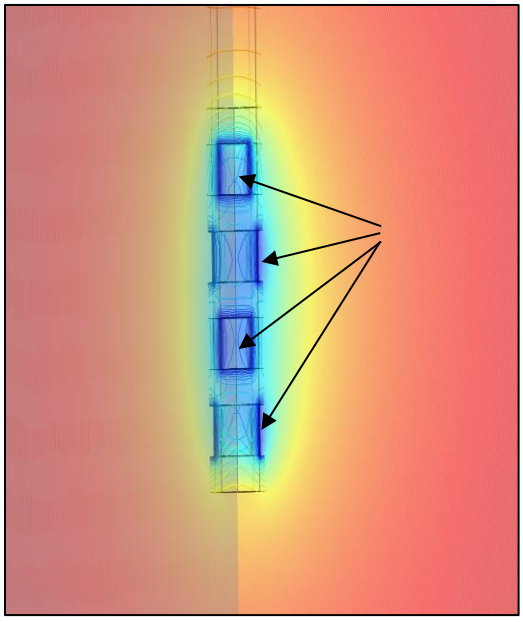

Figure 10: Electric potential plot with irregular configuration, showing which electrodes are active.

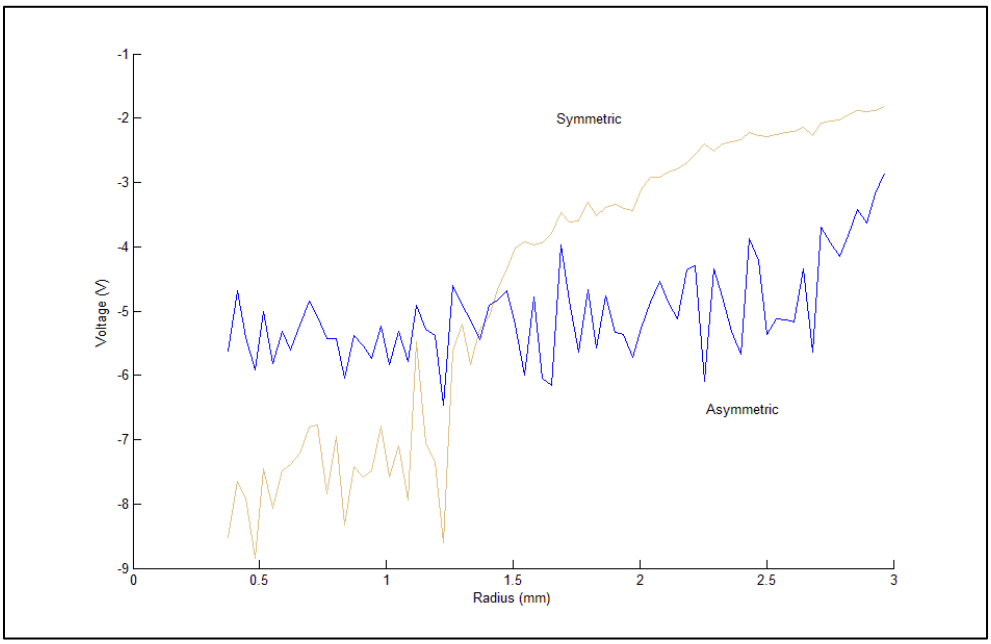

Figure 11. Voltage verses radius: Quantification of the stimulation around the probe in symmetric and asymmetric stimulation.

From the graph above, we gained a good understanding of the effectiveness of selective activation of the probe. It was important to measure the variance in each of the findings in order to better analyze it. Accordingly, we found that the variance in the data for the asymmetric activation was 0.539, compared to 5.32 for symmetric activation of the probe. In this case, a smaller variance corresponds to a smaller voltage gradient in the radial direction. This further supports that the propagation of the potential outward has a smaller potential gradient for the asymmetric when compared to the symmetric probe, suggesting more uniform stimulation across a larger area of the nearby brain tissue.

CONCLUSION AND DESIGN RECOMMENDATIONS

Our results indicate that the temperature profile around the probe can be highly selective depending on the desired asymmetric activation of the probe. Voltage application of -1.561 V_{rms} is believed to be sufficient to cause stimulation of the surrounding brain tissue. Stimulation can reach up to 2.5 mm away from the probe in the brain tissue or spread less than 2 mm away, depending on how the activation of the probe is directed. No significant temperature increase was observed in the unstimulated direction when the probe was asymmetrically activated. This enables more precise control and steering in deep brain stimulation treatments.

Based on sensitivity analysis, the temperature distribution does not depend significantly on blood perfusion rate, metabolic heat generation, electrical conductivity or thermal conductivity, yet change in voltage significantly affects the temperature distribution. Based on this conclusion, treatment by steering stimulation could be optimized based on each individual patient's needs, aided with a computational model such as the one considered here. This would require obtaining the geometry of a person's brain before treatment and plugging geometry into the computational

model. Being able to model the heat distribution throughout the area around the probe would result in higher precision in controlling potential variations in temperature, and decreased likelihood of brain damage.

A. Constraints

A constraint to our recommendation for personalized treatment based on disc size measurements would be cost and feasibility. It may be difficult to gather specific dimensions needed for input in the model from a CT scan or MRI. Another major constraint is cost. MRIs are very expensive, and are often only used when completely necessary. However, in this case it may be feasible to consider this as an option in order to avoid damaging brain tissue.

B. Model Improvement Recommendations

The model considered was a simplified version of the probe proposed by Martens, *et al* and was used to make analysis and optimization more feasible. It is also more reasonable that a probe of this form will be examined before a full 16X4 array probe: earlier versions of this probe (like the one manufactured in the Martens, *et al* for use in a primate brain) are more likely to be of this form. This, however, can be adjusted, and the COMSOL model for the full probe is pictured in Appendix C, Fig. 3.

It would also be worthwhile to consider treating the brain as inhomogeneous tissue. This, however, is substantially more difficult than treating it as homogeneous is. There is neither the data available nor sufficient consistency in and among brain physiology to expect straightforward improvement in accuracy of the model after including it. It would also be important to consider how the probe may affect the tissue immediately surrounding it outside of this stimulation. Insertion of foreign bodies into tissue can often lead to inflammation of the surrounding tissue, which would change tissue properties. Taking this into account might be an important next step in the accurate modeling of DBS.

Appendix A: Mathematical statement of the problem

A. Mathematics/Equations:

Governing equation (transient):

$$\rho C_p \frac{\partial T}{\partial t} = \nabla(k\nabla T) - \rho_b w_b C_{p,b}(T - T_b) + Q_m + \sigma(\nabla V)^2 \qquad \textbf{Eq. (1)}$$

This equation is solving for the change in temperature of surrounding brain tissue, to ensure the increase of temperature does not cause damage to the surrounding tissue. The increase of temperature is caused by the conduction from the probe, the metabolic heat generated by the stimulated neurons, and the heat generated by the voltage potential. Blood circulating through the brain acts as a heat sink and is considered to be constant throughout the tissue.

The density and specific heat in the first term are estimated properties of homogeneous brain tissue. The heat capacity is a property of the metal used for the probe, and is assumed to be constant through the entire simulation due to the minimal temperature change. Blood properties will be used for the density, perfusion, and specific heat, and are assumed to be constant at body temperature. The metabolic heat generation term was estimated from experimentally back literature and held constant in the model.

The term $(\nabla V)^2$ is solved for by solving Laplace's Equation:

$$\nabla^2 V = 0 \qquad \textbf{Eq. (2)}$$

Time steps used in the heat equation will be sufficiently large so that, in application of pulses, we can take V to be the root mean square voltage.

$V_{rms} = \sqrt{\frac{1}{P}\int_0^P v(t)^2 dt}$, where P is the period of the voltage oscillation. ***Eq. (3)***

The surrounding tissue is assumed to be homogeneous and isotropic, having constant conductivity.

The boundary conditions are:

- T(r=R,t) = body temperature (parameter to be varied in analysis)
- $V(r = R, t) = 0$ (Electric Potential is zero at the boundary), where R is some distance from the center of the probe sufficiently far out, in this case 50 mm.
- T(top and bottom) = Body Temperature = 37°C
- V(top and bottom) = 0V.
- The initial condition is: T(t = 0, r) = body temperature = 37 °C.

B. Input Parameters:

There are different sets of parameters that correspond to different regions, shown in Fig.1.

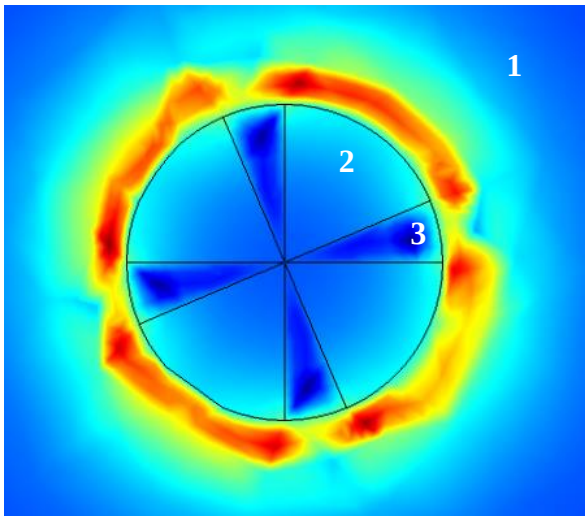

Figure 1: Regions of the model. 1 represents the surrounding brain tissue. 2 is the electrically active part of the probe. 3 is the insulating portions of the probe (found between both rows and columns of the electrodes, as well as in the upper portion of the probe without any electrodes).

The material properties are shown in Table A1, below. For the brain region for which both blood perfusion and metabolic heat generation must be considered, extra terms pertaining to these heat sources will be included.

Table A1. Material and heat source properties pertaining to each domain, obtained from Elwassif, *et al.*

Region 1:

Property	Value
Density of tissue (ρ)	$1040\ \frac{Kg}{m^3}$
Heat capacity of tissue (C_p)	$3650\ \frac{J}{Kg*K}$
Density of blood (ρb)	$1057\ \frac{Kg}{m^3}$
Specific heat of blood (C_p)	$3600\ \frac{J}{Kg*K}$
Blood perfusion rate (ω)	$0.008\ \frac{mL}{s*m^3}$

Blood Temperature (T_b)	36.7 °C
Metabolic heat Gen (Q_m)	9132 $\frac{W}{m^3}$
Thermal conductivity of tissue (κ)	$\frac{W}{m * K}$
Electrical conductivity of tissue (σ)	.25 $\frac{S}{m}$

Region 2:

Property	Value
Density (ρ)	$21560 \frac{Kg}{m^3}$
Heat capacity (C_p)	$134 \frac{J}{Kg * K}$
Thermal Conductivity (κ)	$31 \frac{W}{m * K}$
Electrical conductivity (σ)	$10^7 \frac{S}{m}$

Region 3:

Property	Value
Density (ρ)	$1110 \frac{Kg}{m^3}$
Heat capacity (C_p)	$1500 \frac{J}{Kg * K}$
Thermal Conductivity (κ)	$.026 \frac{W}{m * K}$
Electrical conductivity (σ)	$10^{-10} \frac{S}{m}$

Appendix B: Solution strategy

A. Solver Configuration:

The BDF solver was used to solve the algebraic equations with default settings. Our problem solved over 15 minutes, using a time step of 5 seconds. We noticed that using of 1 seconds created a much longer solution time, but did not change the temperature profile. We used a relative tolerance of 0.01 and an absolute tolerance of 0.0010. These were the default values in COMSOL, and they worked well to solve our problem. Changing the tolerance values also did not change our temperature profile solution.

B. Mesh

Our mesh consisted of 5263 elements. This value was chosen after constructing the mesh convergence plot shown in Figure B1, from which it seems that the temperature profile does not change with the addition of elements beyond 5000. We used the adaptive mesh property in COMSOL to automatically calculate the mesh elements in order to prevent crashing. A comparatively fine mesh was constructed at the surface of the probe (this was done by specifying an adaptive mesh for the boundary) while a significantly coarser mesh was used for the rest of the domain. The mesh is pictured in Figure B2.

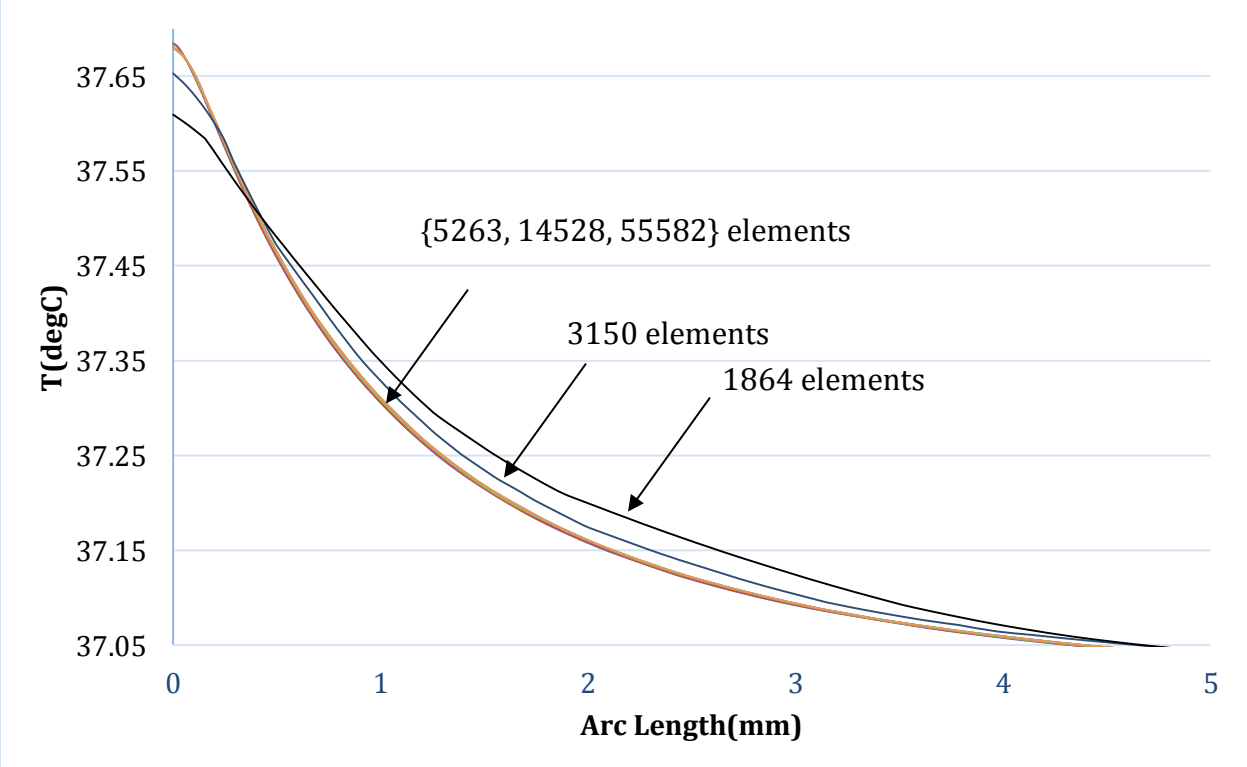

Figure 1. A mesh convergence plot of temperature along the line shown in Figure C1.

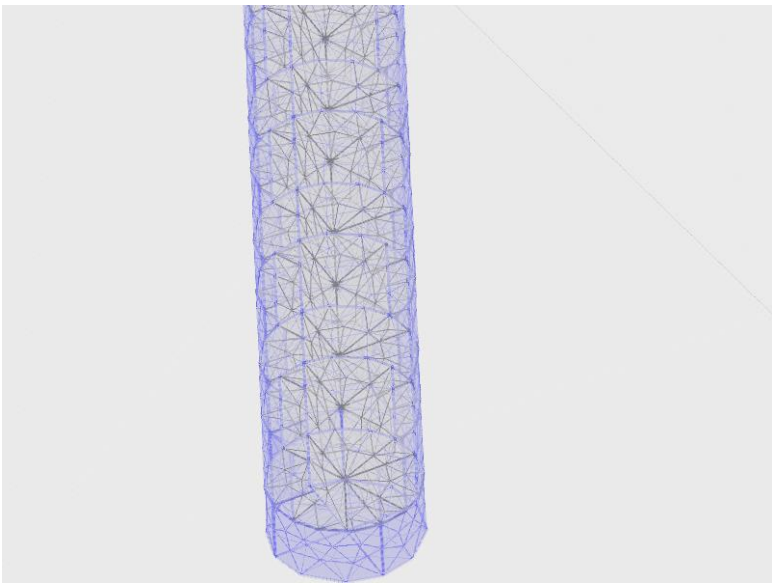

Figure 2. Visual Representation of Mesh.

Appendix C: Additional visuals

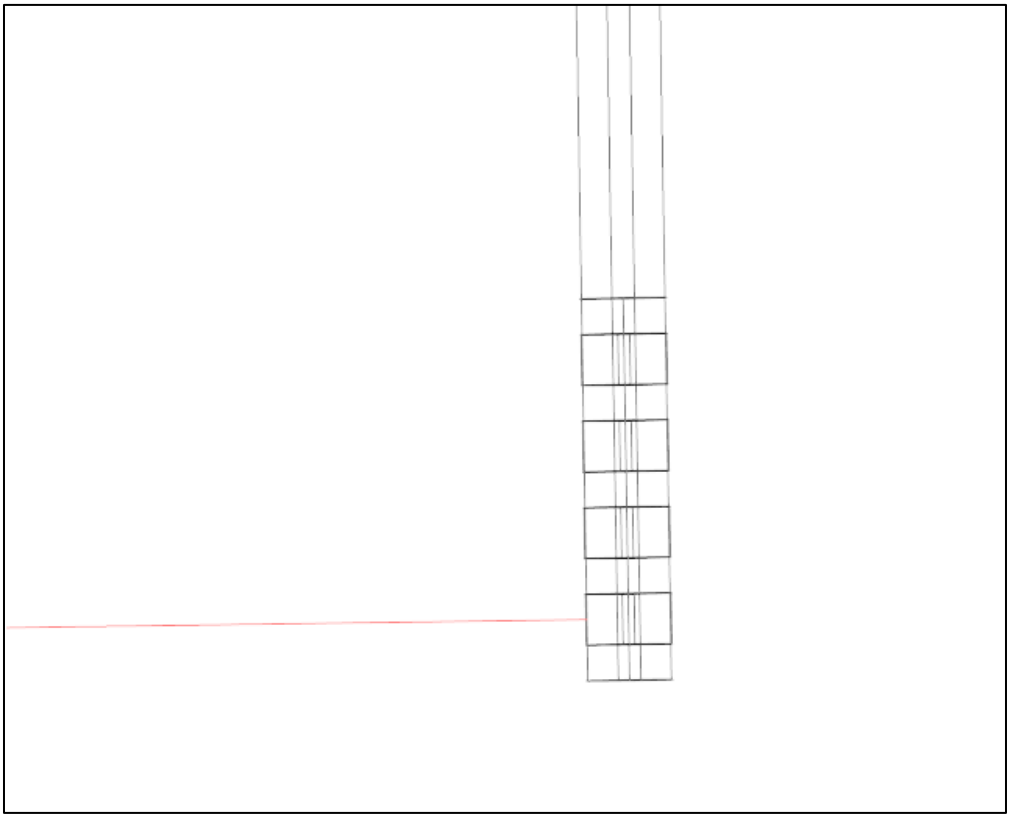

Figure 1: Line along with temperature is calculated in sensitivity analyses.

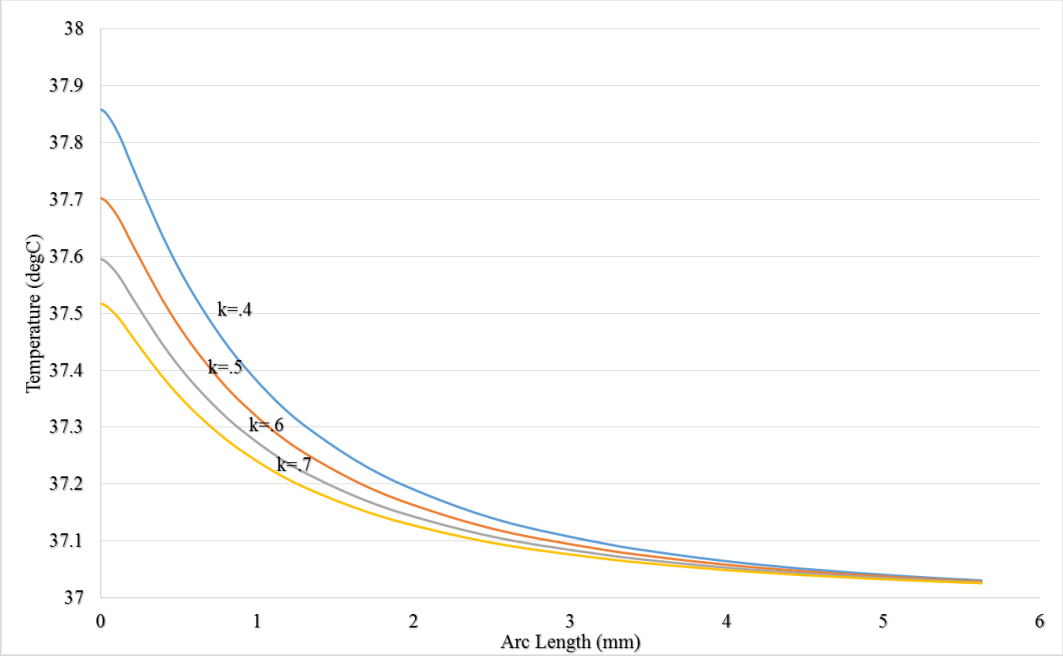
38
37.9
37.8
37.7
37.6
37.5
37.4
37.3
37.2
37.1
37
Temperature (degC)
k=.4
k=.5
k=.6
k=.7
0
1
2
3
4
5
6
Arc Length (mm)

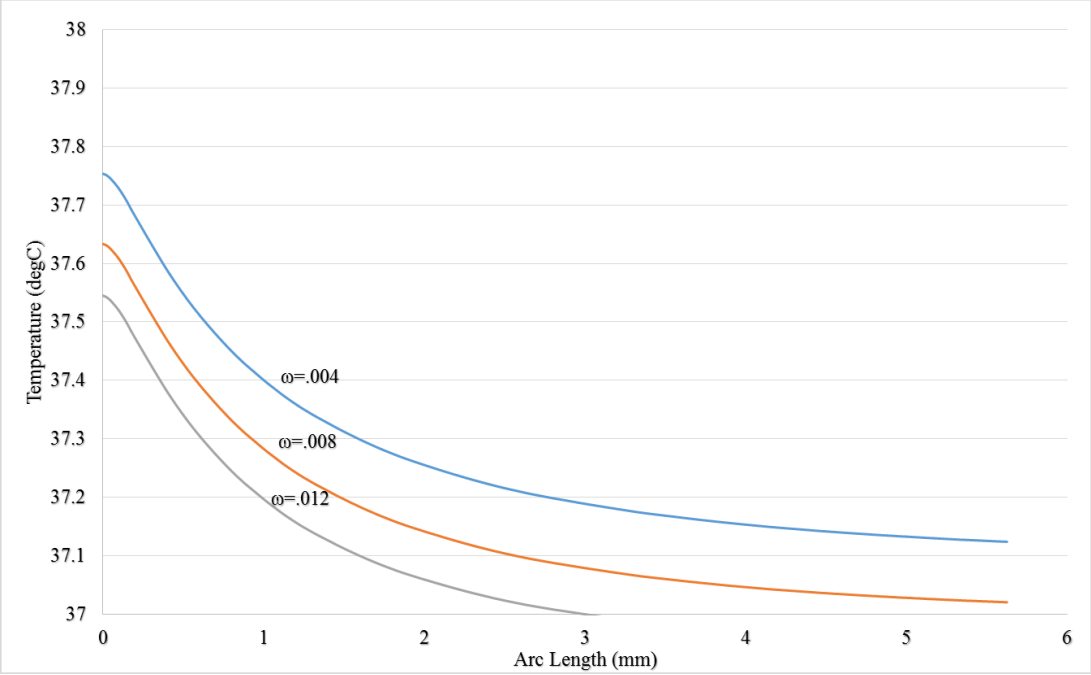
38
37.9
37.8
37.7
37.6
37.5
37.4
37.3
37.2
37.1
37
Temperature (degC)
ω=.004
ω=.008
ω=.012
0
1
2
3
4
5
6
Arc Length (mm)

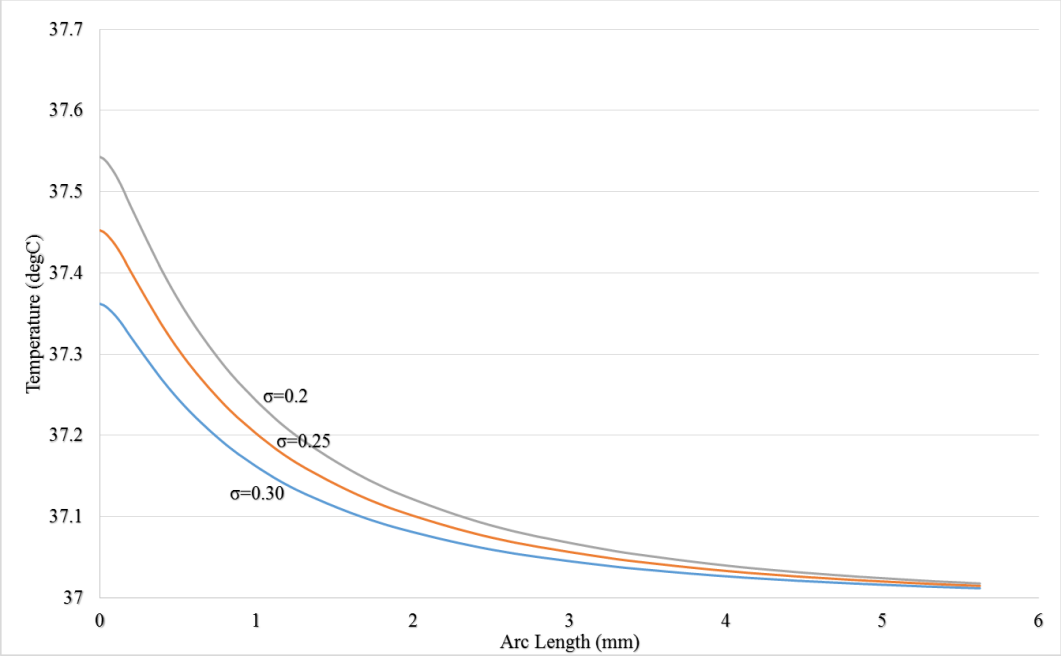

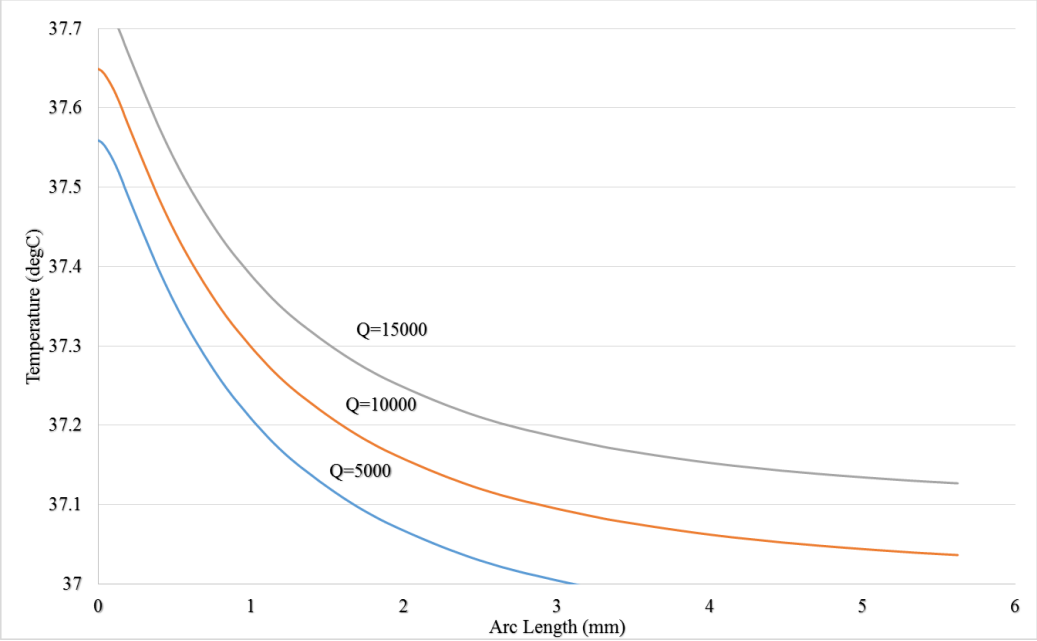

Figure 2: Scaled up versions of sensitivity plots discussed in the sensitivity analysis section.

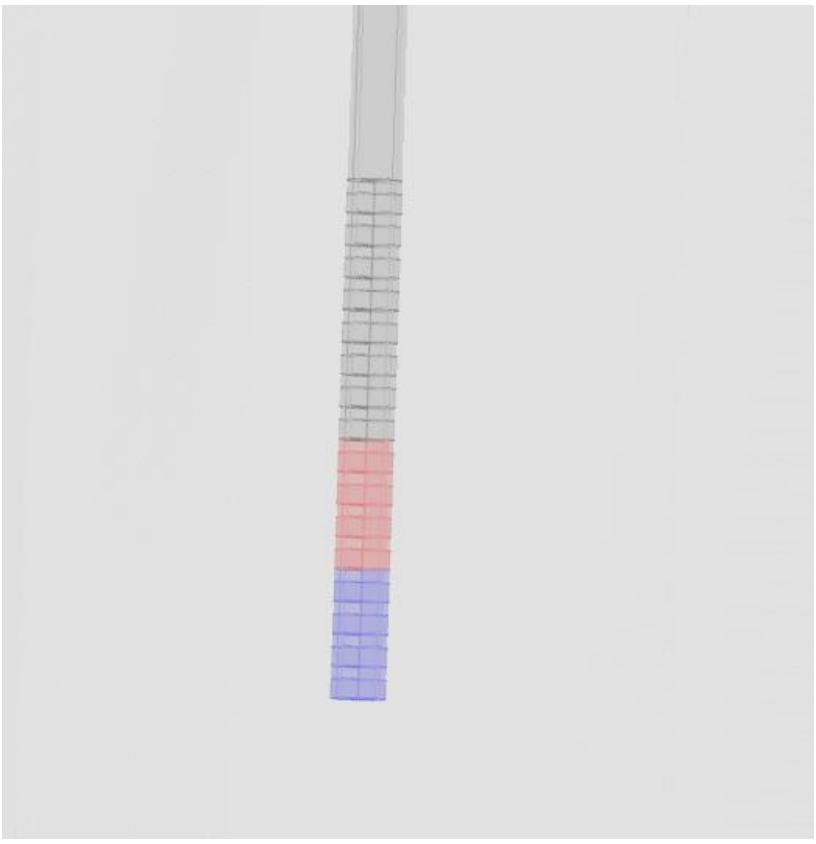

Figure 3: 16x4 expanded probe COMSOL model.

Appendix D:

References

Alexander GE, Crutcher MD (1990) Functional architecture of basal ganglia circuits: neural substrates of parallel processing. *Trends Neurosci,* 13,266–271

Alexander GE, Crutcher MD, DeLong MR (1990) Basal ganglia-thalamocortical circuits: parallel substrates for motor, oculomotor, "prefrontal" and "limbic" functions. *Prog Brain Res,* 85,119–146

Benabid AL, Pollak P, Gervason C, Hoffmann D, Gao DM, et al. 1991. Long-term suppression of tremor by chronic stimulation of the ventral intermediate thalamic nucleus. *Lancet*, 337, 403–6

Breit, S., Schulz, J. B., and Benabid, A. (2004). Deep Brain Stimulation. *Cell and Tissue Research*, 318, 275-88.

Elwassif, M., Kong, Q., Vazquez, M., and Bikson, M. (2006). Bio-heat transfer model of deep brain stimulation-induced temperature changes. *Journal of Neural Engineering,* 3, 306-315.

Kern., D. S., and Kumar, R. (2007). Deep Brain Stimulation. *The Neurologist,* 13, 237-52.

Martens, H.C.F., Toader, E., Decre, M. M. J., Anderson, D. J., Vetter, R., Kipke, D.R., Baker, K. B., Johnson, M. D., and Vitek, J. L. (2011). Spatial steering of deep brain stimulation volumes using a novel lead design. *Clinical Neurophysiology*, 122, 3, 558-566.

Perlmutter, J. S., and Mink., J. W. (2006). Deep Brain Stimulation. *The Annual Review of Neuroscience*, 29, 229-57.